Moving cast shadow detection of vehicle using combined color models

Bangyu Sun[1] and Shutao Li[1]

1. College of Electrical and Information Engineering, Hunan University, Changsha, 410082, China
E-mail: jinjin135@126.com; shutao_li@yahoo.com.cn

Abstract: Moving cast shadow detection of vehicle is important to vehicle detection and tracking. In this paper, a novel moving cast shadow detection approach using combined color models is proposed. Firstly, the ratio of hue over intensity in HSI color model is used to detect the bright object pixels in foreground regions. Secondly, we employ the theory of photometric color invariants in $c_1c_2c_3$ color model to distinguish the dark (similar to shadow) and colorful object pixels from shadow pixels. Finally, to improve the accuracy of shadow detection, post processing is used to correct failed shadow and object detection. Experimental results indicate that the proposed method can detect moving cast shadows accurately.

Key Words: traffic monitoring system, shadow detection, HSI model, post processing

1 INTRODUCTION

Moving objects detection plays an important role in intelligent visual surveillance systems. However, shadows of moving objects often cause serious errors in image analysis because of the misclassification of shadows and moving objects [1]. During the past years, many methods of moving cast shadow detection have been proposed [2] [3] [4] [5]. Generally, shadow detection methods can be divided into two categories: shape-based methods and spectrum-based methods.

Shape-based methods use the priori geometric information for the scenes, objects, and light-source location to solve the shadow detection problem [3]. Hsieh et al. utilized lane features and proposed a line-based algorithm to separate shadows from the moving vehicles [4]. Yoneyama et al. established a two-dimensional joint-vehicle/shadow model to represent the objects and their cast shadows in order to separate the shadows from the objects [6]. Because these methods depend on the geometrical relationship of the objects in the scenes, they lose effectiveness when the geometrical relationship changes.

In the existing shadow detection method, shadow spectral characteristics are more popular than geometric features. Spectrum-based techniques employ spectral information of object regions and shadow regions to detect shadows [7] [8]. Compared with the shape-based approaches, the information based on spectrum-based approaches is more explicit, because the spectral relationship between object regions and shadow regions is affected only by illumination, rather than light source directions or object shapes. In [9], brightness and chromaticity distortions are defined and normalized, so a pixel is separated as shaded background or shadow if it has similar chromaticity but lower brightness than the same background pixel. In [2], Cucchiara et al. proposed an improved shadow detection in moving object detection with HSV color information. In [10], a classification method about color edges applying photometric invariant features into shadow geometry edges, highlight edges and material changes is proposed.

The differences of scenes may result in the difference of the luminance. In addition, the vehicles also have different color, size and speed. Most algorithms can not adapt to these changes well. In this paper, a novel moving cast shadows detection approach using combined color models is proposed. In the first step, the ratio of hue over intensity is employed to determine whether the pixel is a shadow pixel or not. In the second step, three Gaussian models in color model $c_1c_2c_3$ are established to detect shadows. The $c_1c_2c_3$ invariant color features can be adaptive to variable illumination conditions. In the third step, we get the rough result of shadow detection by synthesizing the above two results. Finally, to improve the accuracy of shadow detection, two types of spatial analysis are designed to verify actual shadow pixels. In the process of shadow detection, we deal with the foreground region instead of the whole image, thus it reduces the computation time.

The rest of this paper is organized as follows. Section 2 briefly reviews two color models. Section 3 introduces the process of shadow detection. Experimental results and discussions are provided in Section 4, and the conclusions are drawn in Section 5.

2 TWO COLOR MODELS

In this section, we will introduce the two color models employed in this paper.

2.1 Color model HSI

Because the intensity of shadow region is lower than that of object region, the HSI color model can reflect this problem better than other models, such as RGB, YUV. Here, we apply the ratio of the hue over the intensity. The following equation is aimed to transform RGB into HSI color model.

978-1-4244-7210-9/10/$26.00 ©2010 IEEE

$$\begin{bmatrix} I \\ V_1 \\ V_2 \end{bmatrix} = \begin{bmatrix} \frac{1}{3} & \frac{1}{3} & \frac{1}{3} \\ -\frac{\sqrt{6}}{6} & -\frac{\sqrt{6}}{6} & \frac{\sqrt{6}}{3} \\ \frac{1}{\sqrt{6}} & \frac{-2}{\sqrt{6}} & 0 \end{bmatrix} \begin{bmatrix} R \\ G \\ B \end{bmatrix} \quad (1)$$

$$S = \sqrt{V_1^2 + V_2^2} \quad (2)$$

$$H = \begin{cases} \tan^{-1}(\frac{V_2}{V_1}), & if \ \ V_1 \neq 1 \\ H \text{ is undefined}, & \text{othersise} \end{cases} \quad (3)$$

In the HSI color model, H and I components denote the hue and intensity components respectively.

2.2 Color model $c_1c_2c_3$

A spectral property of shadows can be derived by considering photometric color invariants. Photometric color invariants are functions which describe the color configuration of each image point discounted by shadows and highlights. These functions are demonstrated to be invariant to changes in viewing direction and illumination condition. One of the typical photometric color invariants is color model $c_1c_2c_3$, and $c_1c_2c_3$ is defined as follows [12].

$$\begin{cases} c_1 = \arctan[\frac{R}{\max(G, B)}] \\ c_2 = \arctan[\frac{G}{\max(R, B)}], \\ c_3 = \arctan[\frac{B}{\max(R, G)}] \end{cases} \quad (4)$$

where R, G, B is the corresponding value of red, green, and blue components of a pixel.

3 SHADOW DETECTION

In this section, we employ the two color models mentioned in Section 2 to detect shadows. The process of shadow detection is described as follows.

Step 1: For the spectral characteristics of shadows, we detect shadows in HSI and $c_1c_2c_3$ color models, and then get two shadow images.

Step 2: Getting the rough shadow image by synthesizing the above two images using logical operation.

Step 3: Post processing is used to o correct failed shadow and object detection in order to improve the accuracy of shadow detection.

The block diagram of the proposed shadow detection procedure is illustrated in Fig. 1. Input foreground images are passed through the system and I_i is shadow detection image after each step.

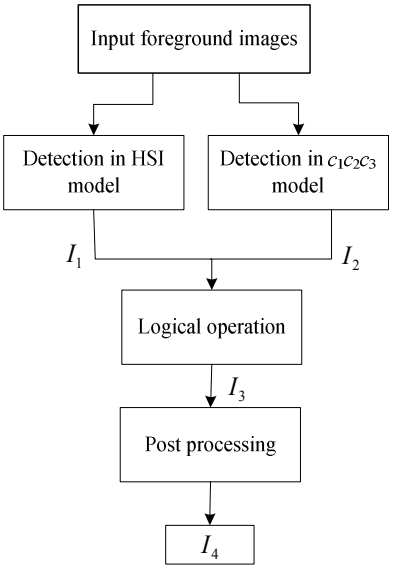

Fig.1 Block diagram of the proposed shadow detection method

3.1 Rough detection

As we all know, the intensity of object region is usually larger that of shadow region, so we can find a threshold to separate shadows from foreground region. When detecting the shadows, we only deal with the foreground region and segment the foreground region into one or more independent connected regions. By employing HSI model, H and I components must be scaled to the range in [0, 1]. In this way, we can get the hue-equivalent image H_e and the intensity-equivalent image I_e, respectively. The ratio r is defined as

$$r(x, y) = \frac{H_e(x, y) + 1}{I_e(x, y) + 1}, \quad (5)$$

where (x, y) is coordinate of a pixel. $H_e(x, y)$ and $I_e(x, y)$ represent the values H_e and I_e at position (x, y), respectively. The term $I_e(x, y) + 1$ can avoid denominator by zero and the $(H_e(x, y) + 1)/(I_e(x, y) + 1)$ ratio shall enhance the hue property of shadows with low luminance. i.e., pixels in shadowed regions will have higher values in the $(H_e(x, y) + 1)/(I_e(x, y) + 1)$ ratio than those pixels in object regions. Then a threshold for each connected region separately can be found to detect shadows. A shadow map can be evaluated by

$$S_1(x, y) = \begin{cases} 1, & r(x, y) > T \\ 0, & \text{otherwise} \end{cases}, \quad (6)$$

where T is a threshold. If $S_1(x, y) = 1$ represents the shadow pixel at (x, y).

In order to get the threshold T, the following equation is exploited.

$$T = \arg\min_T (\sum_{i=0}^{T} P(i)(i - \mu_1)^2 + \sum_{i=T+1}^{255} P(i)(i - \mu_2)^2) \quad (7)$$

where $\mu_1 = \sum_{i=0}^{T}(iP(i)/W_1)$, $\mu_2 = \sum_{i=T+1}^{255}(iP(i)/W_2)$. And $W_1 = \sum_{i=0}^{T}P(i)$, $W_2 = \sum_{i=T+1}^{255}P(i)$, where $P(i)$ is the probability of the ratio value *i* in *r* map.

According to the result, the method above in HSI color model can only distinguish the large intensity pixels from the low intensity pixels. There are still many pixels having the similar low intensity to shadow pixels, e.g. the windshield of a vehicle and the region of object not being irradiated, thus it may mistake the low intensity pixel of the object for shadow pixel. In color model $c_1c_2c_3$ this problem can be solved well.

As mentioned in section II-B, we define the (P_R, P_G, P_B) as follows.

$$\begin{cases} P_R = c_1 - c_1^b \\ P_G = c_2 - c_2^b \\ P_B = c_3 - c_3^b \end{cases}, \quad (8)$$

where c_1^b, c_2^b, c_3^b denote the values of $c_1, c_2\ c_3$ in the background image at the same position, respectively.

In the coordinate systems based on (P_R, P_G, P_B), Gaussian models are exploited to represent the constant (P_R, P_G, P_B). From the RGB ratio Gaussian Shadow Model in [5], we can established three Gaussian models for P_R, P_G, P_B components to detect shadows. The models can be found by analyzing shadow samples taken from the shadow region in an image frame. u_R, u_G, u_B are the mean values and $\sigma_R, \sigma_G, \sigma_B$ are the standard deviation of P_R, P_G, P_B respectively. To cope with the variations, we employ the Gaussian distribution inside $\pm 1.5\sigma$ (88.6%) as a threshold.

$$S_2(x,y) = \begin{cases} 1, & if\ |P_R(x,y) - u_R| < 1.5\sigma_R\ and \\ & |P_G(x,y) - u_G| < 1.5\sigma_G\ and \\ & |P_B(x,y) - u_B| < 1.5\sigma_B \\ 0, & otherwise \end{cases}, \quad (9)$$

where (x,y) is coordinate of a pixel. $P_R(x,y)$, $P_G(x,y)$, and $P_B(x,y)$ are the input values of P_R, P_G, and P_B at position (x,y). If $S_2(x,y) = 1$ represents the shadow pixel at position (x,y).

From the theory in HSI and $c_1c_2c_3$ models, the synthetic result can be represented as follows.

$$S\ (x,y) = \begin{cases} 1, & if\ S_1(x,y) = 1\ and\ S_2(x,y) = 1 \\ 0, & otherwise \end{cases} \quad (10)$$

If $S(x,y) = 1$ represents that the pixel at (x,y) is classified as shadow pixel, otherwise, as object pixel.

3.2 Post processing

Through the procedures of detecting shadows, two types of errors may occur: shadow detection failure and object detection failure. Shadow detection failure means that shadow pixels may be misclassified as moving objects and results from some shadow pixels having the similar informations to the object pixels. This occurs especially at the edges of shadow regions. Object detection failure is that some regions of objects are misclassified as shadows. To increase the accuracy of shadow detection, a post-processing spatial analysis for shadow verification is employed. The spatial analysis is used to confirm the true objects as well as the true shadows according to their geometric properties. The steps of post processing are described as follows.

Step 1- Correct shadow detection failure: In the process of detecting shadows, the true shadows sometimes break into isolated shadow blobs. Usually, the sizes of these shadow blobs are smaller than the detected objects in the sequence. These small blobs are not considered as moving objects. We should eliminate the small shadow blobs from the whole blobs of moving object candidates. So the problem can be easily corrected by morphological close operation.

Step 2-Correct object detection failure: If one part of the detected object is misclassified as a shadow, most of the exterior pixels adjacent to the boundary of this region will be located inside the candidate foregrounds. Given this condition, boundary information can be used to confirm whether the shadow candidate is a true shadow or not. In this paper, each distinct candidate shadow region is determined by using a connected components labeling algorithm. Then, the boundary's exterior 8-neighboring pixels set E are evaluated by equation (11).

$$E = MaskCmpt \oplus SE - MaskCmpt, \quad (11)$$

where $SE = \begin{bmatrix} 1 & 1 & 1 \\ 1 & 1 & 1 \\ 1 & 1 & 1 \end{bmatrix}$. *MaskCmpt* represents the component mask. Symbol $\oplus$ denotes morphological dilation. At last, the number of pixels in the set E (N_E) is counted, as well as the number of the pixels detected as foreground in E (N_M). If the in-equation $N_M > 0.8N_E$ holds, the component will be modified as foreground, otherwise, confirmed as shadow.

4 EXPERIMENTAL RESULTS

This section presents the results of moving cast shadow detection that has been tested in different scenes. Two sequences are used in experiments. Sequence1 is downloaded at http://210.44.184.112/shadowInvCS and derives from a road crossing. Sequence2 comes from Jingzhu Highway. The proposed method is used to compare two well-known methods. Statistical Nonparametric (SNP) [11] approach and Deterministic Nonmodel-Based (DNM) [2] approach are chosen.

4.1 Metrics of performance evaluation

In order to analyze the proposed method objectively and quantitatively, the shadow detection rate η and shadow

discrimination rate ξ are widely used [8]. They are defined as follows.

$$\eta = \frac{TP_S}{TP_S + FN_S}, \qquad \xi = \frac{TP_F}{TP_F + FN_F} \tag{12}$$

In (12), the subscript symbol S stands for shadow and F for foreground, where TP_S and TP_F respectively represent the numbers of shadow pixels and foreground pixels correctly recognized. FN_S and FN_F respectively represent the numbers of shadow pixels and foreground pixels falsely recognized.

4.2 Comparison results

The results of Sequence1 and Sequence2 processed by three algorithms are demonstrated in Fig.2 and Fig.3, and white color corresponds to the detected shadow pixels.

The DNM algorithm works in the HSV color model and is the one with the most stable performance. Due to the limitation of this algorithm, it may not detect the object regions which have the similar intensity to shadows. In Fig.2-b and Fig.3-b, sizable windshields of the vehicles are misclassified as shadows and some other shadows are not extracted correctly. The SNP algorithm treats object colors as a reflectance model from the Lambertian hypothesis. It employs the normalized distortion of brightness and distortion of chrominance, computed from the difference between the background color of a pixel and its value in the current image, to verify whether a pixel is a shadow or not. The SNP algorithm is very effective in most of the scenes, but with very variable performances. It achieves good detection performance in indoor scene, but will be out of work in traffic system. In Fig.2-c and Fig.3-c, there are obvious misclassifications between shadows and objects.

In our proposed method, combined color models are employed to detect shadows. From the purpose in HSI and $c_1c_2c_3$ color models, they are largely complementary. Obviously, the color of vehicles in Sequence1 is different from that in Sequence2, and the algorithm we proposed above can remove shadows efficiently. Meanwhile, the size of moving objects in Sequence2 is different in Sequence1, and the proposed algorithm can also detect the moving shadows exactly. The experimental results show that the proposed method provides more reliable shadow detection results than the two chosen methods.

a) Original image b) DNM

c) SNP d) Proposed method

Figure 2 Comparison results of Sequence1 processed by three methods

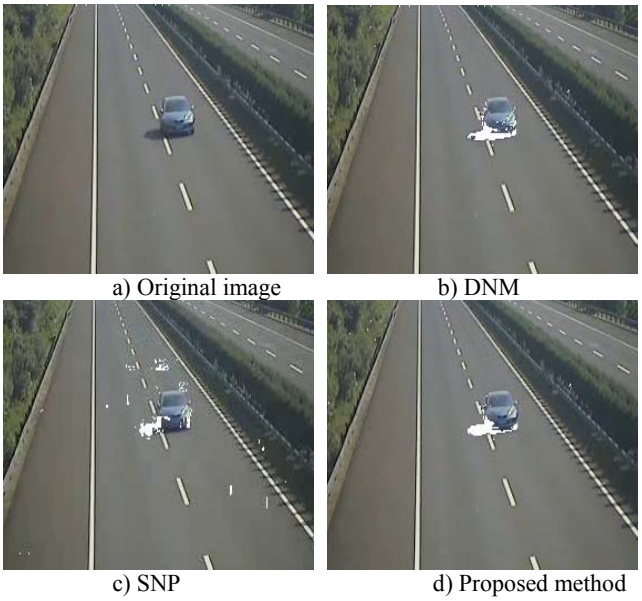

a) Original image b) DNM

c) SNP d) Proposed method

Figure 3 Comparison results of Sequence2 processed by three methods

We have presented a quantitative comparison of our proposed method with the two chosen methods, and the results are shown in Table 1. The results show that the proposed method excels the classical methods.

Table 1: Quantitative evaluation and comparison of the proposed method

	Sequence1		Sequence2	
	η (%)	ξ (%)	η (%)	ξ (%)
DNM	86.8	82.5	85.4	74.6
SNP	70.4	72.6	74.5	82.4
Proposed	88.5	91.6	90.2	89.3

5 CONCLUSIONS

In this paper, a novel method for moving cast shadow detection of vehicle is proposed. By analyzing the shadow information, we employ the combined color models. From the purpose of the methods in these two models, we can see that they are largely complementary. Experimental results show that the proposed method can detect moving cast shadows

accurately, and it outperforms two well-known shadow detection approaches obviously. For the further research of shadow detection, edge information can be used as a feature of the shadow, while the shadow region is smoother than the object region. In addition, some potential properties of shadows will be further investigated to make systems more accurate and effective.

ACKNOWLEDGEMENTS

This paper is supported by the National Natural Science Foundation of China (No. 60871096 and 60835004), the Ph.D. Programs Foundation of Ministry of Education of China (No. 200805320006), the Key Project of Chinese Ministry of Education (2009-120), and the Open Projects Program of National Laboratory of Pattern Recognition.

REFERENCES

[1] E. Salvador, A. Cavallaro, T. Ebrahimi. Cast shadow segmentation using invariant color features. *Computer Vision and Image Understanding*, 2(95): 238-259, 2004.

[2] Rita. Cucchiara, Costantino. Grana, M. Piccardi, Andrea Prati and Stefano Sirotti. Improving Shadow Suppression in Moving Object Detection with HSV Color Information. *Proc. ICITS*, Oakland (CA), USA, 2001, pp: 334-339.

[3] J-W. Hsieh, W-F. Hu, C-J. Chang, Y-S. Chen. Shadow elimination for effective moving object detection by Gaussian shadow modeling. *Image and Vision Computing*, 21(2): 505-516, 2003.

[4] J-W. Hsieh, S-H. Yu, Y-S. Chen, W-F. Hu. A shadow elimination method for vehicle analysis. *Proc. ICPR*, Cambridge, UK, 2004, Vol. 4, pp. 372-375.

[5] K-T Song, J-C Tai. Image-based traffic monitoring with shadow suppression. *Proceedings of the IEEE*, 95(2): 413-426, 2007.

[6] A. Yoneyama, C. H. Yeh, and C. C. J. Kuo. Moving cast shadow elimination for robust vehicle extraction based on 2-D joint vehicle/shadow models. *Proc. ICAVSBS*, Miami, FL, 2003, pp. 21-22.

[7] S. Nadimi and B. Bhanu. Physical models for moving shadow and object detection in video. *IEEE Trans. Pattern Anal. Mach. Intell.*, 26(8): 1079-1087, 2004.

[8] A. Prati, I. Mikic, M. M. Trivedi, and R. Cucchiara. Detecting moving shadows: Algorithms and evaluation. *IEEE Trans. Pattern Anal. Mach. Intell.*, 25(7): 918-923, 2003.

[9] Pankaj Kumar, Kuntal Sengupta and Adrian Lee. A Comparative Study of Different Color Spaces for Foreground and Shadow Detection for Traffic Monitoring System. *Proc. ICITS*, Singapore, 2002, pp.100-105.

[10] T. Gevers, H. Stokman. Classifying color edges in video into shadow-geometry, highlight, or material transitions. *IEEE Trans. Multimedia*, 5(2): 237-243, 2003.

[11] I. Haritaoglu, D. Harwood, and L. S. Davis. W4: Real-time surveillance of people and their activities. *IEEE Trans. Pattern Anal. Mach. Intell.*, 22(8): 809-830, 2000.

[12] T. Gevers, A. W. M. Color-based object recognition. *Pattern Recognition*, 32(3): 453-464, 1999.

[13] R. Cucchiara, C. Grana, M. Piccardi, and A. Prati. Detecting moving objects, ghosts and shadows in video streams. *IEEE Trans. Pattern Anal. Mach. Intell*, 25(10): 1337-1342, 2003.

[14] Martel-Brisson, N. Zaccarin. A. Moving Cast Shadow Detection from a Gaussian Mixture Shadow Model. *Proc. CVPR*, 2005, Vol. 2, pp.643-648.

[15] V. J. D. Tsai. A comparative study on shadow compensation of color aerial images in invariant color models. *IEEE Trans. Geosci. Remote Sens.*, 44(6): 1661-1671, 2006.